UC San Diego

UC San Diego Previously Published Works

Title

Traceless synthesis of ceramides in living cells reveals saturation-dependent apoptotic effects

Permalink

https://escholarship.org/uc/item/8h07p6jd

Journal

Proceedings of the National Academy of Sciences of the United States of America, 115(29)

ISSN

0027-8424

Authors

Rudd, Andrew K

Devaraj, Neal K

Publication Date

2018-07-17

DOI

10.1073/pnas.1804266115

Peer reviewed

eScholarship.org Powered by the California Digital Library
University of California

Traceless synthesis of ceramides in living cells reveals saturation-dependent apoptotic effects

Andrew K. Rudd[a] and Neal K. Devaraj[a,1]

[a]Department of Chemistry and Biochemistry, University of California, San Diego, La Jolla, CA 92093

Edited by David M. Chenoweth, University of Pennsylvania, Philadelphia, PA, and accepted by Editorial Board Member Stephen J. Benkovic June 13, 2018 (received for review March 11, 2018)

Mammalian cells synthesize thousands of distinct lipids, yet the function of many of these lipid species is unknown. Ceramides, a class of sphingolipid, are implicated in several cell-signaling pathways but poor cell permeability and lack of selectivity in endogenous synthesis pathways have hampered direct study of their effects. Here we report a strategy that overcomes the inherent biological limitations of ceramide delivery by chemoselectively ligating lipid precursors in vivo to yield natural ceramides in a traceless manner. Using this method, we uncovered the apoptotic effects of several ceramide species and observed differences in their apoptotic activity based on acyl-chain saturation. Additionally, we demonstrate spatiotemporally controlled ceramide synthesis in live cells through photoinitiated lipid ligation. Our in situ lipid ligation approach addresses the long-standing problem of lipid-specific delivery and enables the direct study of unique ceramide species in live cells.

ceramide | apoptosis | sphingolipids | chemoselective | lipids

Ceramides are produced within the cell through both de novo synthesis and salvage pathways and carry out diverse cellular functions (1). Natural ceramide levels play an integral role in insulin resistance (2), endosomal sorting pathways (3), gene regulation (4), and programmed cell death (5). They are also implicated in tumor suppression and methods for their cellular delivery could be attractive as cancer therapeutics (6). Despite considerable interest in the biological function of ceramides, direct study of their effects in vivo is limited by their impermeability to the cell membrane. As a result, current methods often rely on the use of unnatural short-chain ceramides. These analogs exhibit increased cell permeability but behave differently than natural ceramides in both physical membrane properties (7) and biological activity (8). Testing how *N*-fatty acyl structure affects ceramide function is also not possible using short-chain analogs. Additionally, manipulation of native ceramide metabolism genetically or with inhibitors is limited by the broad substrate selectivity of endogenous ceramide synthases (9). Recently, caged ceramides have been developed for the delivery of ceramide to macrophages but their biological activity, and efficacy in other cell lines, has not been reported (10).

We developed a strategy to overcome these problems by synthesizing native ceramides in situ using two cell-permeable and chemoselective ligation partners. Previously, a salicylaldehyde ester-induced reaction has been reported for peptide ligation which relies on a C-terminal salicylaldehyde and N-terminal serine to selectively generate a peptide linkage (11). This method, however, requires organic solvent, high reactant concentrations, and removal of the salicylaldehyde group under acidic conditions. As an alternative, we sought to develop fatty acid salicylaldehyde esters that react selectively under physiological conditions with the sphingolipid backbone sphingosine to yield natural ceramides. Based on previous observations in our laboratory, we hypothesized that the organization of these reaction partners within membranes would accelerate the modest reaction rate of the salicylaldehyde-mediated ligation (12, 13). Furthermore, functionalizing the phenyl ring of the salicylaldehyde group with electron-donating groups could increase the aqueous stability of the fatty acid ester and eliminate the need for organic solvent.

Results and Discussion

To determine the feasibility of this approach, we synthesized a small collection of palmitic acid salicylaldehyde esters with different ring substituents, **1**–**3**, and performed ligation experiments in the presence of phospholipid vesicles as a model membrane. Upon incubation of 500 μM of palmitic acid salicylaldehyde ester with 250 μM sphingosine at 37 °C in PBS (pH 7.4), C16:0 ceramide was formed within hours (*SI Appendix*, Fig. S1). The salicylaldehyde group is released spontaneously during the reaction, resulting in the traceless formation of ceramide, without the introduction of any extraneous chemical moieties (Fig. 1*A*). From these initial experiments, we found that compound **3** offered superior hydrolytic stability, showing very little degradation (<2%) over 16 h (Fig. 1*B*). Therefore, we chose to employ **3** as a sphingosine ligation partner in a method we term traceless ceramide ligation (TCL).

To investigate the chemoselectivity of this ligation we performed TCL in the presence of two potentially competing biomolecules, serine (Fig. 1*C*) or lyso-sphingomyelin (Fig. 1*D*). Serine possesses the same 2-aminoethanol moiety as sphingosine but is water-soluble. Lysosphingomyelin is localized in the membrane but has only a free amine and not the terminal 2-aminoethanol functionality found in sphingosine. Under these conditions, TCL proceeded with no observable decrease in yield or reaction rate, suggesting that both the terminal 2-aminoethanol functionality and localization in the phospholipid membrane are necessary for ligation. To determine if TCL could occur in live cells, we used

Significance

Ceramides are a chemically diverse class of sphingolipids that have critical roles in a wide range of biological pathways. Despite their high biological interest, ceramides have been difficult to study because of their impermeability to the cell membrane. We overcome the principal issues with ceramide delivery by chemoselectively ligating lipid precursors in vivo. Our method employs a proximity-induced ligation which allows for the in situ synthesis of several different natural ceramide species within live cells. Using this approach, we directly confirm the proapoptotic effects of C16:0 ceramide in vivo and observe that ceramide saturation plays a determinant role in ceramide-driven apoptosis.

Author contributions: A.K.R. and N.K.D. designed research; A.K.R. performed research; A.K.R. analyzed data; and A.K.R. and N.K.D. wrote the paper.

The authors declare no conflict of interest.

This article is a PNAS Direct Submission. D.M.C. is a guest editor invited by the Editorial Board.

Published under the PNAS license.

[1]To whom correspondence should be addressed. Email: ndevaraj@ucsd.edu.

This article contains supporting information online at www.pnas.org/lookup/suppl/doi:10.1073/pnas.1804266115/-/DCSupplemental.

Published online July 2, 2018.

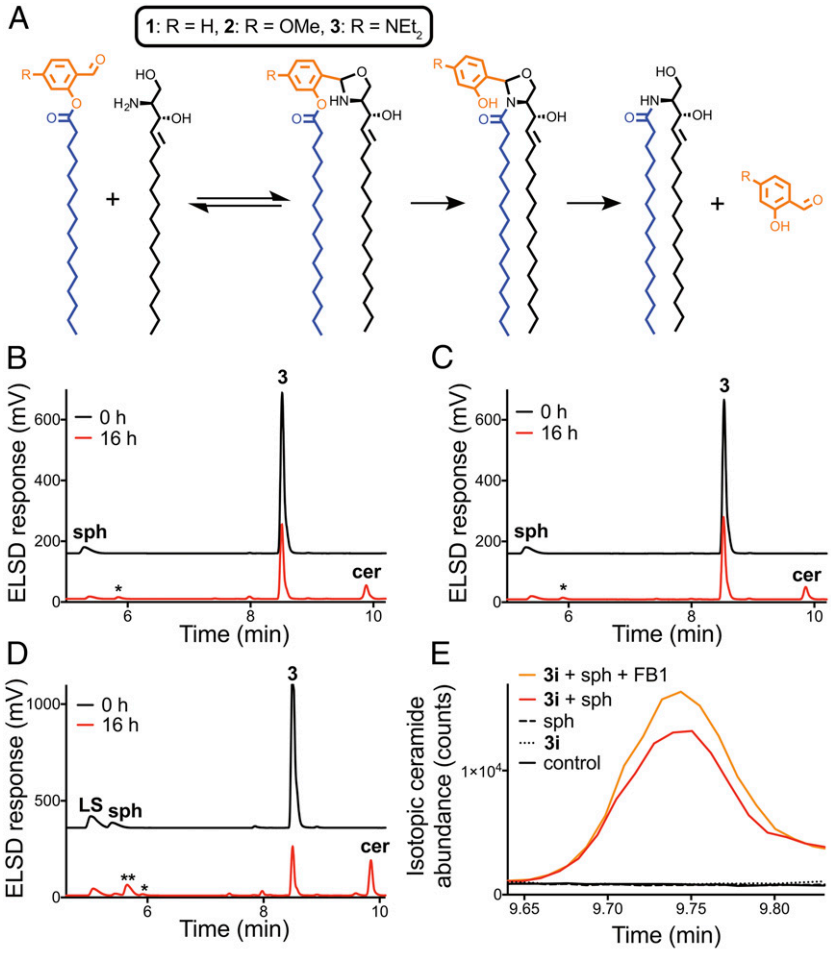

Fig. 1. Fatty acid salicylaldehyde esters and sphingosine react chemoselectively in model membranes and live cells. (*A*) Proposed reaction mechanism for TCL. (*B*) Sphingosine (sph) and **3** in model membranes react to form ceramide (cer) at 37 °C, pH 7.4 over a period of 16 h. (*C* and *D*) The reaction between sph and **3** forms cer chemoselectively in the presence of serine (*C*) and lyso-sphingomyelin (*D*). The production of a small quantity of reversibly formed byproduct **b1** (*) (*B–D*) and **b2** (**) (*D*) is also detected (*SI Appendix*, Fig. S2). (*E*) Isotopic palmitic acid salicylaldehyde ester **3i** reacts with sph within live HeLa cells to form cer detectable in the crude mitochondrial cell fraction.

a ^{13}C isotopic derivative of **3**, **3i**. HeLa cells were incubated in the presence of sphingosine, **3i**, or sphingosine and **3i** combined for 16 h and then lysed. Cell fractionation was used to obtain crude mitochondrial fractions and enrich for the ceramide product formed in internal membranes (14) (*SI Appendix*, Fig. S3). MS analysis detected TCL-synthesized ceramide in the crude mitochondrial fraction only when both ligation partners were added to cells but not when they were added separately. Notably, we could not detect any TCL-synthesized ceramide when cells were treated with **3i** alone. This suggests that endogenous levels of sphingosine are insufficient for TCL. Additionally, the reaction was performed in the presence of an inhibitor of all six ceramide synthases, fumonisin B1 (FB1), which we determined was nonreactive toward **3** (*SI Appendix*, Fig. S4). Under these conditions, the isotopic ceramide product was still observed, confirming that it is not a metabolic product of **3i** (15) (Fig. 1*E*). By performing a whole-cell lipid extraction (16), we determined the total level of ^{13}C-labeled ceramide produced in HeLa cells by TCL to be 136 ± 23 pmol/10^6 cells, indicating that physiological levels of ceramide can readily be synthesized in situ (*SI Appendix*, Fig. S5) (17).

Having confirmed the reaction proceeds in living cells, we investigated whether ceramide-induced apoptosis could be effected by TCL (5, 6). Certain ceramide species, most notably C16:0 ceramide, are known to increase in concentration during apoptosis (18, 19). Evidence suggesting that increases in levels of certain ceramides can directly trigger apoptosis is based on studies utilizing unnatural short-chain ceramides. These nonnative ceramides exhibit substantial differences in structure, solubility, lipid ordering effects, and intracellular diffusion, raising concerns about the validity of these conclusions (20, 21). To test whether we could use TCL to study the apoptotic effects of natural C16:0 ceramide in cells, we incubated cultured HeLa cells in the presence of 100 μM **3** and varying concentrations of sphingosine. Cell viability was not impacted by **3** alone, but incubation with **3** and sphingosine together resulted in significantly lower cell viability compared with the same concentration of sphingosine alone (Fig. 2*A*). Exogenous addition of 100 μM C16:0 ceramide had no effect on cell viability, highlighting the substantial increase in ceramide delivery through in situ TCL, and providing further evidence that TCL occurs intracellularly. Additionally, to confirm that the decrease in viability is due to TCL and not the metabolism of sphingosine to ceramide, we performed the same cell viability assay in the presence of FB1 and observed the same decrease in cell viability when cells were treated with **3** and sphingosine together compared with sphingosine alone (*SI Appendix*, Fig. S6). Visual quantification of cell death (Fig. 2*B*) and fluorescent detection of caspase 3/7 activity (Fig. 2*C* and *SI Appendix*, Fig. S7) confirmed that C16:0 ceramide delivered via TCL results in the activation of apoptotic

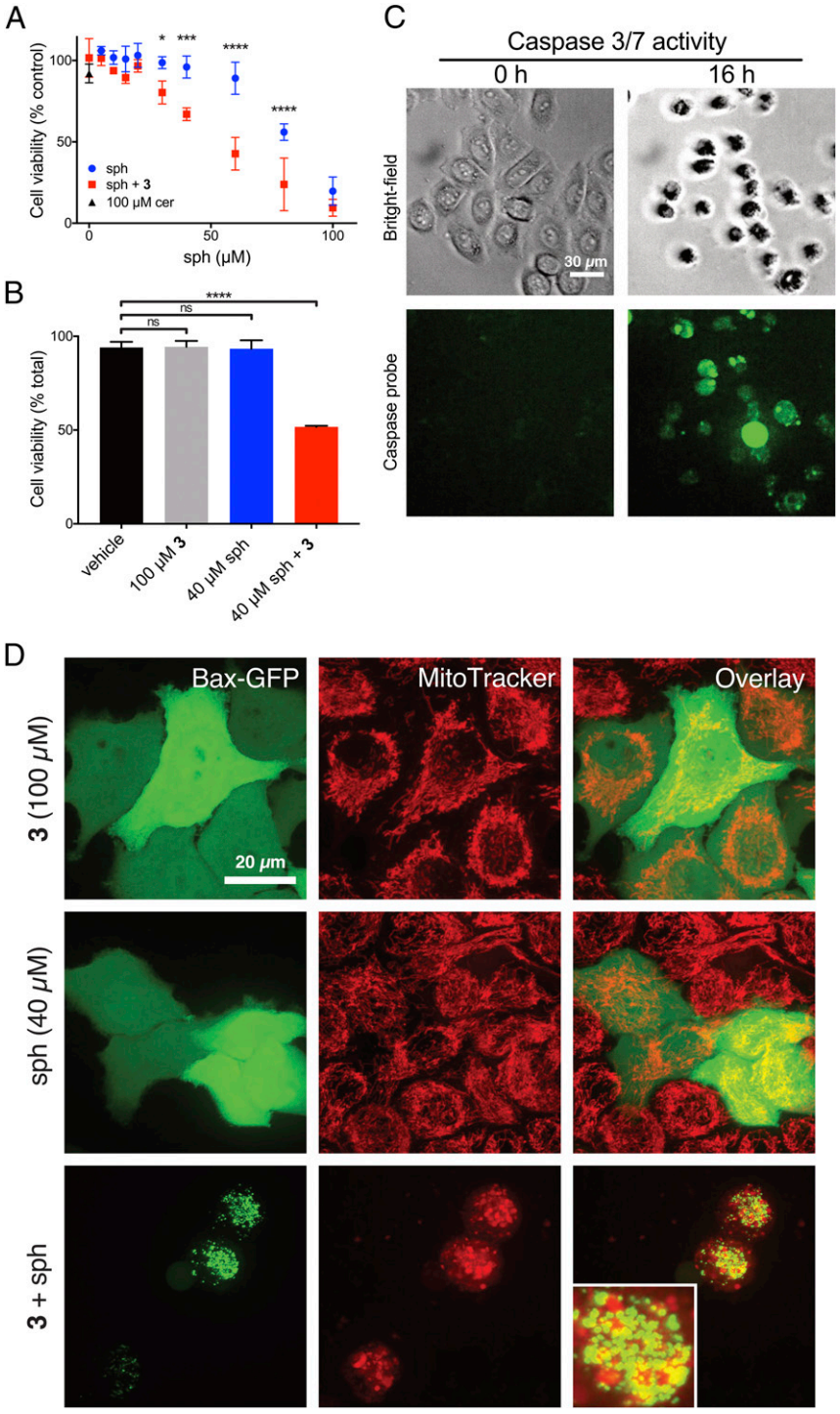

Fig. 2. TCL in live cells triggers apoptosis. (*A* and *B*) Treatment of cultured HeLa cells with 100 μM **3** and sph results in significantly more cell death than sph alone as monitored by a WST-1 proliferation assay (*A*) and total live cell count (*B*). Viability assays were performed in three biological replicates and shown as means ± SD. Statistically significant differences between points at a given sph concentration (*A*) or condition (*B*) are indicated: $*P < 0.05$, $***P < 0.001$, $****P < 0.0001$. ns, not significant. (*C*) Treatment of HeLa cells with 100 μM **3** and 40 μM sph results in the activation of caspases necessary for apoptosis. (*D*) Production of C16:0 ceramide during TCL triggers translocation of Bax-GFP from the cytosol to mitochondria during apoptosis (images in *D* are maximum intensity Z-projections).

caspases. To determine if TCL is compatible with cell lines other than HeLa cells, we performed the same viability experiments using NIH 3T3 cells (*SI Appendix*, Fig. S8). Again, we observed significantly lower cell viability in cells treated with **3** and sphingosine compared with **3** or sphingosine alone.

C16:0 ceramide is hypothesized to exert its proapoptotic function through the recruitment of the protein Bax to the mitochondria, which in turn triggers mitochondrial membrane permeabilization and eventual cell death (22–24). This model, however, is based on a correlation between increased levels of

cellular ceramide and Bax association with the mitochondria (23), or studies using unnatural short-chain ceramides (25). Therefore, it remains unclear if C16:0 ceramide is an effector of Bax translocation in vivo. To determine whether an intracellular increase in C16:0 ceramide alone is sufficient to trigger Bax recruitment to mitochondria, we transiently expressed a Bax-GFP fusion protein in HeLa cells and observed the localization of Bax-GFP with respect to the mitochondrial staining dye MitoTracker. TCL-driven synthesis of C16:0 ceramide within cells resulted in Bax-GFP transitioning to a punctate distribution which partially colocalized to the mitochondria, consistent with previous reports of Bax localization during apoptosis (26, 27) (Fig. 2*D* and *SI Appendix*, Fig. S9). These results demonstrate that increases in intracellular C16:0 ceramide can directly trigger Bax translocation and suggest that this lipid plays a central role in Bax-induced apoptosis.

Cells produce numerous ceramide species with various *N*-fatty acyl groups (28). Ceramides may exert differing biological effects depending on their acyl-chain functionality (1). Analyzing the roles of specific ceramide species is often confounded by the presence of six individual endogenous ceramide synthases (CerS1–6), which produce multiple ceramide products varying in both chain length and degree of unsaturation (9). Additionally, many ceramide species are produced by more than one ceramide synthase, further hindering their study through traditional biochemical methods (9, 28). TCL offers the capability to deliver individual and specific ceramides to cells, something not possible through manipulation of cellular metabolism. As a proof of concept, we synthesized salicylaldehyde esters with differing fatty acid substituents **4**, **5**, and **6** and confirmed that they react with sphingosine to yield a range of ceramide products (*SI Appendix*, Fig. S10). We then generated the different ceramides in living HeLa cells and studied the effect of ceramide structure on cell viability. Delivery of fully saturated C16:0 or C18:0 ceramide using TCL resulted in a significant reduction in cell viability compared with the sphingosine control (Fig. 3 *A* and *B*). In contrast, we observed no reduction in cell viability when monounsaturated C18:1 or C24:1 ceramide was delivered (Fig. 3 *C* and *D*). Differences in chain length did not affect the intracellular delivery of the precursors, as there was no significant difference in cellular levels of C16:0 and C18:1 ceramide formed after addition of sphingosine and isotopic salicylaldehyde esters **3i** and **4i** (*SI Appendix*, Fig. S11). We hypothesized that the observed difference in apoptotic activity of different ceramide species may be due to their ability to promote translocation of Bax to the mitochondria. To test this, we used TCL to synthesize C16:0 and C24:1 ceramide in HeLa cells expressing Bax-GFP. We found that Bax localized to the mitochondria significantly more when cells were treated with C16:0 ceramide (95 ± 2% of cells) than when they were exposed to C24:1 ceramide (10 ± 6% of cells) (Fig. 3 *E* and *F* and *SI Appendix*, Fig. S12). Our results suggest that ceramide saturation plays a determinant role in the apoptotic activity of the molecule and support the hypothesis that ceramide-enriched membrane domains, formed preferentially by saturated ceramides, are required for the recruitment of Bax to the mitochondria and the activation of apoptosis pathways (1, 23, 29).

Ceramide formation is stringently controlled in both time and space (30). We sought to achieve a similar level of control using our ligation strategy. Previously, light-reactive photocages have been developed for the protection and photoinitiated deprotection of biological lipids including sphingosine and ceramide (31–33). While photocaged ceramide is an exceptional tool for the study of ceramide in model membranes (33), it has seen limited application in biological systems (10). Modifying a previous synthetic scheme, we successfully synthesized a coumarin-photocaged analog of sphingosine, **9**. We found that this compound was stable in HeLa cell lysate (*SI Appendix*, Fig. S13) and, upon UV exposure, was uncaged to yield sphingosine with a half-life of 10.6 s (*SI Appendix*, Fig. S14). We used the efficient uncaging and stability of this compound to spatiotemporally control ceramide synthesis in a live cell system. To determine the effect of **9** uncaging in cells, we cultured HeLa cells expressing Bax-GFP as a marker of apoptosis and then exposed them to a range of concentrations of the compound **9** (0–300 μM) and irradiated multiple regions of the cell culture with 405-nm laser and imaged over 10 h (*SI Appendix*, Fig. S15). We chose to use 50 μM **9** for TCL experiments because it did not result in significant cell death after irradiation but, based on cell viability experiments (Fig. 2*A*), should provide a level of sphingosine sufficient for TCL. We cultured HeLa cells expressing Bax-GFP and then incubated them in the presence of 100 μM **3** and 50 μM **9**. Using laser scanning microscopy, we uncaged **9** in a single cell using the 405-nm laser line and then imaged over a period of 12 h. We found that after 10 h only the cell in which **9** was uncaged

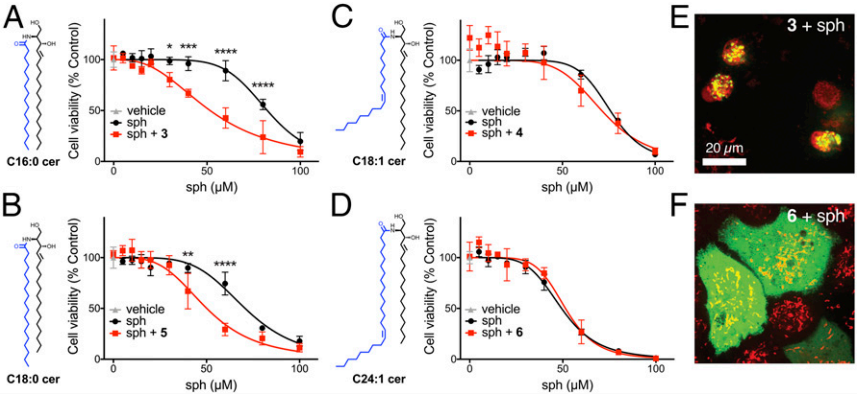

Fig. 3. TCL delivery of specific ceramide species reveals an *N*-acyl chain saturation-dependent effect on cell viability and Bax localization. (*A*–*D*) Viability of cultured HeLa cells after 16-h incubation with TCL precursors as monitored by a WST-1 viability assay. Treatment of cells with 100 μM **3** (*A*) or 100 μM **5** (*B*) and sph results in significantly more cell death than sph alone. Cells treated with 100 μM **4** (*C*) or 100 μM **6** (*D*) and sph or sph alone show no significant difference in cell viability. Viability assays were performed in three biological replicates and shown as means ± SD. Statistically significant differences between points at a given sph concentration are indicated: $*P < 0.05$, $**P < 0.01$, $***P < 0.001$, $****P < 0.0001$. Lines represent a normalized dose–response curve with variable slope. (*E* and *F*) Composite images of Bax-GFP (green) and MitoTracker (red) after treatment with 100 μM **3** or **6** and 40 μM sph for 16 h. Generation of C16:0 ceramide within HeLa cells promotes translocation of Bax-GFP to the mitochondria (*E*), while synthesis of C24:1 ceramide has no effect on Bax-GFP localization (*F*) (images are maximum intensity Z-projections).

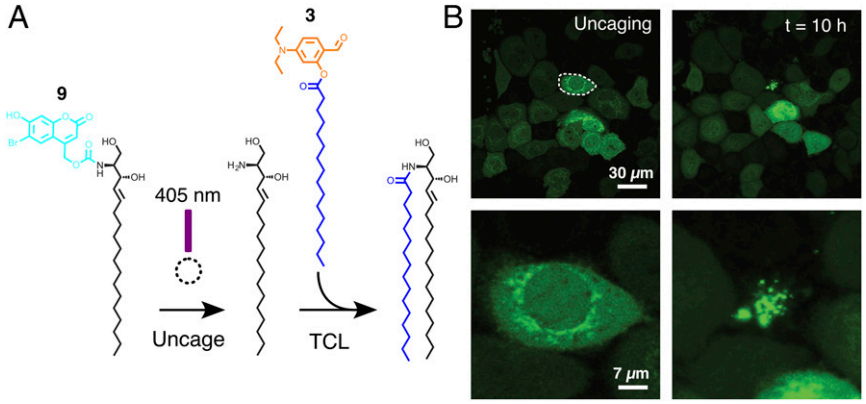

Fig. 4. Photocontrolled initiation of TCL. (*A*) Photocaged sphingosine **9** can be uncaged by 405-nm laser light to produce sph and trigger TCL. (*B*) HeLa cells expressing Bax-GFP were incubated with 100 μM **3** and 50 μM **9**. A single cell in the frame was exposed to 405-nm laser within the outlined area (*Left*) and the sample imaged over a period of 12 h. After 10 h, only the cell in which ceramide synthesis was triggered showed cell death and mitochondrial Bax localization characteristic of C16:0 ceramide-induced apoptosis (*Right*) (t = 10 h; images are maximum intensity Z-projections).

underwent apoptosis, evidenced by the shrinkage of the membrane and punctate Bax-GFP localization (Fig. 4). Controls in which cells were incubated with **3** or **9** separately, and single cells irradiated under the same conditions, showed no apoptosis over the same period (*SI Appendix*, Fig. S16). To determine if this same behavior occurred when **9** was uncaged in multiple cells, we treated HeLa cells under the same conditions as before but irradiated multiple cells in several regions of the chamber slide. As expected, we found that irradiation of cells treated with **3** and **9** resulted in significantly more cell death than irradiation of cells treated with **9** alone (*SI Appendix*, Fig. S17). Furthermore, we found that when cells were treated with precursors which form the unsaturated C24:1 ceramide (100 μM **6** and 50 μM **9**) and then irradiated under the same conditions, there was no significant difference in cell death compared with cells treated with **9** alone (*SI Appendix*, Fig. S17). Spatiotemporally controlled TCL allows for the delivery of ceramides in a cell-selective manner. This could allow for modulation of specific ceramide levels in defined cells or regions of an organism and help to uncover the roles of ceramide in development (34), neurodegeneration (35), and cancer (6).

Conclusions

In conclusion, we have implemented an in situ synthesis scheme for the direct study of ceramides in vivo. Our method enables controlled delivery of specific, full-length ceramides to cells, which is necessary for understanding their specific biological effects. TCL has allowed us to investigate the role of C16:0 ceramide in apoptosis and demonstrate that ceramide saturation is an important modulator of ceramide-driven apoptosis. Future studies using TCL will prove helpful in understanding the metabolism of in situ generated ceramides and their effects on endogenous lipid levels. Furthermore, application of our approach to other lipids may facilitate the study of this often intractable class of biomolecules.

Methods

Chemical Synthesis. Synthetic protocols and compound characterization including MS, ^{1}H NMR, and ^{13}C NMR are available in *SI Appendix*.

Synthesis of Large Unilamellar Vesicles. Large unilamellar vesicles (LUVs) were prepared using a standard extrusion method (36) (full details are available in *SI Appendix*).

TCL in LUVs. To a solution of 5 mM 1,2-dioleoyl-*sn*-glycero-3-phosphocholine LUVs was added sphingosine (as a 40 mM solution in MeOH) to a final concentration of 250 μM and **1**, **2**, **3**, **4**, **5**, or **6** (as a 20 mM solution in l-butanol) to a final concentration of 500 μM. The reaction was incubated at 37 °C in a water bath and 10-μL aliquots were taken at specified times for HPLC analysis [Eclipse Plus C8 column (50 or 75 mm), 0–7 min, 50–95% MeOH in water, 7 min–end, 95% MeOH in water].

MS Detection of TCL in Vivo. HeLa cells, maintained in DMEM (10% FBS and 1% penicillin/streptomycin) were plated in 6-cm culture dishes and grown to confluency at 37 °C, 5% CO_2. Once confluent, media was removed and then the appropriate volume of DMEM (10% FBS and 1% penicillin/streptomycin) was added to achieve a final volume of 3 mL media per dish after addition of reaction components. Where indicated, FB1 was added to a final concentration of 25 μM in 3 mL media. Components of the ligation reaction were prepared as 500 μM solutions in DMEM by diluting stock organic solutions (sphingosine: 40 mM in MeOH and **3i** and **4i**: 20 mM in l-butanol). The **3i** and **4i** were added to a final concentration of 100 μM in designated plates and the cells incubated at 37 °C, 5% CO_2 for 4 h, after which sphingosine was added to a final concentration of 50 μM in designated plates. Cells were then incubated for 16 h at 37 °C, 5% CO_2. After incubation, cells were detached from their culture dish using a plastic cell scraper and the cell suspension (~3 mL) was pelleted by centrifugation at 400 x *g* for 5 min. Supernatant was removed and the cell pellets were resuspended in 1 mL fractionation buffer (250 mM sucrose, 20 mM Hepes, pH 7.4, 10 mM KCl, 1.5 mM $MgCl_2$, 1 mM EDTA, and 1 mM EGTA). Cells were lysed using a Dounce homogenizer and the lysate was transferred to a 1.7-mL Eppendorf tube. When indicated, a cell fractionation was performed on the lysate to isolate the crude mitochondrial fraction (*SI Appendix*). Lipids were extracted from lysate or cell fractions using the Bligh and Dyer method (16). Lipid extracts were analyzed by LC (Eclipse Plus C8 column, 0–7 min, 50–95% MeOH in water, 7–12 min, 95% MeOH in water) to an Agilent 6100 Series Single Quadrapole MS (Agilent Technologies) running in selected ion monitoring mode for the isotopic ceramide peaks ($[M+H]^+$ = 542.5, isotopic C16:0 ceramide) or ($[M+H]^+$ = 582.6, isotopic C18:1 ceramide) (full details are available in *SI Appendix*).

Viability Assays. WST-1, trypan blue, and caspase assays were performed according to the manufacturer's protocols (full details are available in *SI Appendix*).

Bax Localization Experiments. HeLa cells, maintained in DMEM (10% FBS, 1% penicillin/streptomycin, without phenol red) (Thermo Fisher) were plated in an eight-well Lab-Tek chamber slide (Sigma-Aldrich) at a density of 32,000 cells per well and allowed to attach overnight. Cells were transfected with hBax C3-EGFP (Addgene plasmid no. 19741), a gift from Richard Youle (Bethesda, MD), using lipofectamine 2000 (Thermo Fisher) according to the manufacturer's protocol. Components of the ligation reaction were added as described above and cells incubated for 16 h at 37 °C, 5% CO_2. Cells were then treated with MitoTracker Red CMXRos (Thermo Fisher) according to the manufacturer's protocol and imaged using microscopy method A (*SI Appendix*).

Photoactivated TCL. HeLa cells transiently expressing Bax-EGFP were prepared as before. Components of the ligation reaction were prepared as 500 μM solutions in DMEM by diluting stock organic solutions (**9**: 20 mM in MeOH, **3**: 20 mM in l-butanol). Media was removed and then the appropriate volume of DMEM (10% FBS, 1% penicillin/streptomycin, without phenol red) was

added to achieve a final volume of 500 μL media per well after addition of reaction components. Then, **3** was added to a final concentration of 100 μM in designated wells and the cells were incubated at 37 °C, 5% CO_2 for 4 h, after which **9** was added to a final concentration of 50 μM in designated wells and cells were incubated at 37 °C, 5% CO_2 for 1 h. Cells were then maintained at 37 °C, 5% CO_2 during imaging and photoactivation using microscopy method B (*SI Appendix*).

ACKNOWLEDGMENTS. This work was supported by NSF Grant CHE-1254611 and NIH Grants DP2DK111801 and CA009523.

1. Grösch S, Schiffmann S, Geisslinger G (2012) Chain length-specific properties of ceramides. *Prog Lipid Res* 51:50–62.
2. Chavez JA, Summers SA (2012) A ceramide-centric view of insulin resistance. *Cell Metab* 15:585–594.
3. Trajkovic K, et al. (2008) Ceramide triggers budding of exosome vesicles into multivesicular endosomes. *Science* 319:1244–1247.
4. Montefusco DJ, et al. (2013) Distinct signaling roles of ceramide species in yeast revealed through systematic perturbation and systems biology analyses. *Sci Signal* 6: rs14.
5. Pettus BJ, Chalfant CE, Hannun YA (2002) Ceramide in apoptosis: An overview and current perspectives. *Biochim Biophys Acta* 1585:114–125.
6. Morad SAF, Cabot MC (2013) Ceramide-orchestrated signalling in cancer cells. *Nat Rev Cancer* 13:51–65.
7. Sot J, Goñi FM, Alonso A (2005) Molecular associations and surface-active properties of short- and long-N-acyl chain ceramides. *Biochim Biophys Acta* 1711:12–19.
8. Ogretmen B, et al. (2002) Biochemical mechanisms of the generation of endogenous long chain ceramide in response to exogenous short chain ceramide in the A549 human lung adenocarcinoma cell line. Role for endogenous ceramide in mediating the action of exogenous ceramide. *J Biol Chem* 277:12960–12969.
9. Mullen TD, Hannun YA, Obeid LM (2012) Ceramide synthases at the centre of sphingolipid metabolism and biology. *Biochem J* 441:789–802.
10. Kim YA, Ramirez DMC, Costain WJ, Johnston LJ, Bittman R (2011) A new tool to assess ceramide bioactivity: 6-bromo-7-hydroxycoumarinyl-caged ceramide. *Chem Commun (Camb)* 47:9236–9238.
11. Li X, Lam HY, Zhang Y, Chan CK (2010) Salicylaldehyde ester-induced chemoselective peptide ligations: Enabling generation of natural peptidic linkages at the serine/threonine sites. *Org Lett* 12:1724–1727.
12. Brea RJ, Cole CM, Devaraj NK (2014) In situ vesicle formation by native chemical ligation. *Angew Chem Int Ed Engl* 53:14102–14105.
13. Brea RJ, Bhattacharya A, Devaraj NK (2017) Spontaneous phospholipid membrane formation by histidine ligation. *Synlett* 28:108–112.
14. Wieckowski MR, Giorgi C, Lebiedzinska M, Duszynski J, Pinton P (2009) Isolation of mitochondria-associated membranes and mitochondria from animal tissues and cells. *Nat Protoc* 4:1582–1590.
15. Merrill AH, Jr, van Echten G, Wang E, Sandhoff K (1993) Fumonisin B1 inhibits sphingosine (sphinganine) N-acyltransferase and de novo sphingolipid biosynthesis in cultured neurons in situ. *J Biol Chem* 268:27299–27306.
16. Bligh EG, Dyer WJ (1959) A rapid method of total lipid extraction and purification. *Can J Biochem Physiol* 37:911–917.
17. Thomas RL, Jr, Matsko CM, Lotze MT, Amoscato AA (1999) Mass spectrometric identification of increased C16 ceramide levels during apoptosis. *J Biol Chem* 274: 30580–30588.
18. Osawa Y, et al. (2005) Roles for C16-ceramide and sphingosine 1-phosphate in regulating hepatocyte apoptosis in response to tumor necrosis factor-alpha. *J Biol Chem* 280:27879–27887.
19. Mesicek J, et al. (2010) Ceramide synthases 2, 5, and 6 confer distinct roles in radiation-induced apoptosis in HeLa cells. *Cell Signal* 22:1300–1307.
20. Kolesnick RN, Goñi FM, Alonso A (2000) Compartmentalization of ceramide signaling: Physical foundations and biological effects. *J Cell Physiol* 184:285–300.
21. van Blitterswijk WJ, van der Luit AH, Veldman RJ, Verheij M, Borst J (2003) Ceramide: Second messenger or modulator of membrane structure and dynamics? *Biochem J* 369:199–211.
22. Pastorino JG, et al. (1999) Functional consequences of the sustained or transient activation by Bax of the mitochondrial permeability transition pore. *J Biol Chem* 274: 31734–31739, and erratum (2000) 275:8262.
23. Lee H, et al. (2011) Mitochondrial ceramide-rich macrodomains functionalize Bax upon irradiation. *PLoS One* 6:e19783.
24. Taha TA, Mullen TD, Obeid LM (2006) A house divided: Ceramide, sphingosine, and sphingosine-1-phosphate in programmed cell death. *Biochim Biophys Acta* 1758: 2027–2036.
25. von Haefen C, et al. (2002) Ceramide induces mitochondrial activation and apoptosis via a Bax-dependent pathway in human carcinoma cells. *Oncogene* 21:4009–4019.
26. Wolter KG, et al. (1997) Movement of Bax from the cytosol to mitochondria during apoptosis. *J Cell Biol* 139:1281–1292.
27. Hou Q, et al. (2011) Mitochondrially targeted ceramides preferentially promote autophagy, retard cell growth, and induce apoptosis. *J Lipid Res* 52:278–288.
28. Mullen TD, et al. (2011) Selective knockdown of ceramide synthases reveals complex interregulation of sphingolipid metabolism. *J Lipid Res* 52:68–77.
29. Pinto SN, Silva LC, Futerman AH, Prieto M (2011) Effect of ceramide structure on membrane biophysical properties: The role of acyl chain length and unsaturation. *Biochim Biophys Acta* 1808:2753–2760.
30. Holthuis JCM, Menon AK (2014) Lipid landscapes and pipelines in membrane homeostasis. *Nature* 510:48–57.
31. Luo J, et al. (2014) Genetically encoded optochemical probes for simultaneous fluorescence reporting and light activation of protein function with two-photon excitation. *J Am Chem Soc* 136:15551–15558.
32. Höglinger D, et al. (2015) Intracellular sphingosine releases calcium from lysosomes. *eLife* 4:e10616.
33. Ramirez DMC, Pitre SP, Kim YA, Bittman R, Johnston LJ (2013) Photouncaging of ceramides promotes reorganization of liquid-ordered domains in supported lipid bilayers. *Langmuir* 29:3380–3387.
34. Bieberich E (2011) Ceramide in stem cell differentiation and embryo development: Novel functions of a topological cell-signaling lipid and the concept of ceramide compartments. *J Lipids* 2011:610306.
35. Cutler RG, et al. (2004) Involvement of oxidative stress-induced abnormalities in ceramide and cholesterol metabolism in brain aging and Alzheimer's disease. *Proc Natl Acad Sci USA* 101:2070–2075.
36. Mayer LD, Hope MJ, Cullis PR (1986) Vesicles of variable sizes produced by a rapid extrusion procedure. *Biochim Biophys Acta* 858:161–168.